

Published in final edited form as:

Nat Methods. 2013 June ; 10(6): 515–523. doi:10.1038/nmeth.2477.

Mapping brain circuitry with a light microscope

Pavel Osten¹ and Troy W. Margrie^{2,3}

¹Cold Spring Harbor Laboratory, One Bungtown Road, Cold Spring Harbor, NY 11724, USA

²Department of Neuroscience, Physiology and Pharmacology, University College London, Gower Street, London WC1E 6BT, United Kingdom

³Division of Neurophysiology, The MRC National Institute for Medical Research, Mill Hill, London NW7 1AA, United Kingdom

Abstract

The beginning of the 21st century has seen a renaissance in light microscopy and anatomical tract tracing that together are rapidly advancing our understanding of the form and function of neuronal circuits. The introduction of instruments for automated imaging of whole mouse brains, new cell type-specific and transsynaptic tracers, and computational methods for handling the whole-brain datasets has opened the door to neuroanatomical studies at an unprecedented scale. We present an overview of the state of play and future opportunities in charting long-range and local connectivity in the entire mouse brain and in linking brain circuits to function.

Since the pioneering work of Camillo Golgi and Santiago Ramón y Cajal at the turn of the last century^{1,2}, advances in light microscopy (LM) and neurotracing methods have been central to the progress in our understanding of anatomical organization in the mammalian brain. The discovery of the Golgi silver-impregnation method allowed the visualization of neuron morphology, providing the first evidence for cell type- and connectivity-based organization in the brain. The introduction of efficient neuroanatomical tracers in the second half of the century greatly increased the throughput and versatility of neuronal projection mapping, which led to the identification of many anatomical pathways and circuits, and revealed the basic principles of hierarchical and laminar connectivity in sensory, motor and other brain systems^{3,4}.

The beginning of this century has seen a new period of method-driven renaissance in neuroanatomy, one that is distinguished by the focus on large-scale projects generating unprecedented amounts of anatomical data. Instead of the traditional “cottage industry” approach of studying one anatomical pathway at a time, the new projects aim to generate complete datasets—so-called projectomes and connectomes—that can be used by the scientific community as resources for answering specific experimental questions. These efforts range in scale and resolution from the macroscopic—studies of the human brain by magnetic resonance imaging (MRI), to the microscopic—dense neural circuit reconstructions of small volumes of brain tissue by electron microscopy (EM) (see accompanying reviews in this issue by Michael Milham and colleagues and Moritz Helmstaedter, respectively)^{5,6}.

Corresponding authors. PO: osten@cshl.edu, TWM: tmargri@nimr.mrc.ac.uk.

Competing Financial Interests

PO declares competing interests.

TWM has no competing interests.

Advancements in LM methods, the focus of our review, are being applied to the mapping of point-to-point connectivity between all anatomical regions in the mouse brain by means of sparse reconstructions of using anterograde and retrograde tracers⁷. Taking advantage of the automation of LM instruments, powerful data processing pipelines, and combinations of traditional and modern viral vector-based tracers, teams of scientists at Cold Spring Harbor Laboratory (CSHL), Allen Institute for Brain Science (AIBS), and University of California Los Angeles (UCLA) are racing to complete a connectivity map of the mouse brain—dubbed the “mesoscopic connectome”—which will provide the scientific community with online atlases for viewing entire anatomical datasets⁷. These efforts demonstrate the transformative nature of today’s LM-based neuroanatomy and the astonishing speed with which large amounts of data can be disseminated online and have an immediate impact on research in neuroscience laboratories around the world.

As the mouse mesoscopic connectomes are being completed, it is clear that LM methods will continue to impact the evolution of biological research and specifically neuroscience: new transsynaptic viral tracers are being engineered to circumvent the need to resolve synapses, which has constrained the interpretation of cell-to-cell connectivity in LM studies, and new assays combining anatomical and functional measurements are being applied to bridge the traditional structure-function divide in the study of the mammalian brain. This review aims to provide an overview of today’s state of the art in LM instrumentation and to highlight the opportunities for progress as well as the challenges that need to be overcome in order to transform neuronal tracing studies into a truly quantitative science yielding comprehensive descriptions of long-range and local projections and connectivity at the level of whole mouse brains. We also discuss current strategies for the integration of anatomy and function in the study of mouse brain circuits.

Automated light microscopes for whole brain imaging

The field of neuroanatomy has traditionally been associated with labor-intensive procedures that greatly limited the throughput of data collection. Recent efforts to automate LM instrumentation have standardized and dramatically increased the throughput of anatomical studies. The main challenge for these methods is to maintain the rigorous quality of traditional neuroanatomical studies, resulting from detailed visual analysis, careful data collection and expert data interpretation.

There are currently two alternative approaches to automation of LM for imaging three-dimensional (3D) whole-brain datasets, one based on the integration of block-face microscopy and tissue sectioning, the other based on light-sheet fluorescence microscopy (LSFM) of chemically cleared tissue. The first approach has been developed for wide-field imaging, line-scan imaging, and confocal and two-photon microscopy^{8–16}. Common to all these instruments is the motorized movement of the sample under the microscope objective for top view mosaic imaging, followed by mechanical removal of the imaged tissue before the next cycle of interleaved imaging and sectioning steps (Figure 1 a and b). Since the objective is always near the tissue surface, it is possible to use high numerical aperture (NA) lenses to achieve submicron resolution close to the diffraction limits of LM.

Three instruments have been designed that combine two-photon microscopy¹⁷ followed by tissue sectioning by either ultra-short laser pulses in all-optical histology¹⁰, milling machine in two-photon tissue cytometry¹², or vibrating blade microtome in serial two-photon tomography (STP tomography)¹⁵ (Figure 1a). Whereas in both all-optical histology and two-photon tissue cytometry the sectioning obliterates the imaged tissue, the integration of vibratome-based sectioning in STP tomography allows the collection of the cut tissue for further analysis by, for example, immunohistochemistry (see below). In addition, the tissue

preparation by simple formaldehyde fixation and agar embedding in STP tomography has minimal detrimental effects on fluorescence and brain morphology. This makes STP tomography applicable to a broad range of neuroanatomical projects utilizing genetically encoded fluorescent protein-based tracers, which are sensitive to fixation, dehydration and tissue clearing conditions. This method is also versatile in terms of the mode and resolution of data collection. For example, imaging the mouse brain as a dataset of 280 serial coronal sections, evenly spaced at 50 μm and at xy resolution 1 μm , takes about ~21 hours and generates a brain atlas-like dataset of ~70 GB (gigabytes). A complete visualization can be achieved by switching to 3D scanning of z -volume stacks between the mechanical sectioning steps, which allows the entire mouse brain to be imaged, for instance, at 1 μm xy and 2.5 μm z resolution in ~8 days, generating ~1.5 TB (terabytes) of data¹⁵. The instrument is commercially available from TissueVision Inc. (Cambridge, MA). The Allen Brain Institute is using this methodology for its Mouse Connectivity project (see below).

Two instruments have been designed to combine bright-field line-scan imaging and ultra-microtome sectioning of resin-embedded tissue in methods named knife-edge scanning microscopy (KESM)¹³ and micro-optical sectioning tomography (MOST)¹⁴ (Figure 1b). The latter was used to image Golgi-stained mouse brain at $0.33 \times 0.33 \times 1.0 \mu\text{m}$ x - y - z resolution, generating >8 TB of data in ~10 days^{13,14}. The MOST instrument design was also recently built for fluorescent imaging (fMOST) by confocal laser scanning microscopy, with the throughput of one mouse brain at 1.0 μm voxel resolution in ~19 days¹⁶. The KESM imaging is now also available as a commercial service from 3Scan (San Francisco, CA).

The second, alternative, approach for automated whole-brain imaging is based on light-sheet fluorescence microscopy (also known as selective-plane illumination microscopy or SPIM¹⁸ and ultramicroscopy¹⁹) (Figure 1c). This approach allows fast imaging of chemically cleared “transparent” mouse brains without the need for mechanical sectioning^{19,20}, but, at least until now, with some trade-offs for anatomical tracing applications. The chemical clearing procedures reduced the signal of fluorescent proteins, but this problem appears to be solved by a new hydrogel-based tissue transformation and clearing method called CLARITY²¹ (see perspective by Karl Deisseroth about this methodology in this focus²²). The spatial resolution of LSFM for the mouse brain has also been limited by the requirement for large field of view objectives with low power and low NA that were used for the visualization of the whole brain^{19,23}. However, new objectives with long working distance (WD) and high NA, such as 8 mm WD / 0.9 NA objective from Olympus, promise to enable LSFM of the whole mouse brain at submicron resolution. If necessary, LSFM can also be combined with one of several forms of structured illumination (SI) to reduce out-of-focus background fluorescence and improve contrast^{24–26}. Taken together, these modifications are likely to enhance the applicability of LSFM to anterograde tracing of thin axons at high resolution in the whole mouse brain, as done by STP tomography in the AIBS Mouse Connectivity project (see below) and by fMOST in a recent report¹⁶. In addition, LSFM is well suited for retrograde tracing in the mouse brain, which relies on detection of retrogradely fluorescently labeled neuronal somas that are typically > 10 micron in diameter. Such application was recently demonstrated for mapping retrograde connectivity of granule cells of the mouse olfactory bulb²⁰ using rabies viruses that achieve high levels of fluorescent protein labeling^{27,28}.

Mesoscopic connectivity-mapping projects

The labeling of neurons and subsequent neuroanatomical tract tracing by LM methods has been used for over a century to interrogate the anatomical substrate of information transmission in the brain. Throughout those years, the credo of neuroanatomy “The gain in

brain is mainly in the stain” meant to signify that progress was made mainly through the development of new anatomical tracers. Yet, despite the decades of neuroanatomical research, the laborious nature of tissue processing and data visualization kept the progress in our knowledge of brain circuitry at a disappointingly slow pace⁷. Today, neuroanatomy stands to greatly benefit from the application of high-throughput automated LM instruments and powerful informatics tools for the analysis of mouse brain data^{29,30}. The high-resolution capacity LM methods afford, and the fact that an entire brain dataset can be captured, makes these systems well-suited for systematic charting of the spatial profile and connectivity of populations of neurons and even individual cells projecting over long distances.

The pioneering effort in the field of anatomical projects applied at the scale of whole animal brains was the Allen Mouse Brain Atlas of Gene Expression, which catalogued *in situ* hybridization maps of more than 20,000 genes in an online 3D digital mouse brain atlas^{29,31,32}. The proposal by a consortium of scientists led by Partha Mitra (CSHL) to generate similar LM-based atlases of “brainwide neuroanatomical connectivity” in several animal models⁷ has in short time spurred three independent projects, each promising to trace all efferent and afferent anatomical pathways in the mouse brain. The Mitra team’s Mouse Brain Architecture Project (<http://brainarchitecture.org>) at CSHL aims to image >1000 brains, the Allen Mouse Brain Connectivity Atlas project (<http://connectivity.brain-map.org>) led by Hongkui Zeng at AIBS plans for >2000 brains, and the Mouse Connectome Project (www.mouseconnectome.org) led by Hong-Wei Dong at UCLA plans for 500 brains, each brain injected with 4 tracers. While the CSHL and UCLA projects use automated wide-field fluorescence microscopy (Hamamatsu Nanozoomer 2.0 and Olympus VS110) to image manually sectioned brains, the Mouse Connectivity project at the Allen Institute is being done entirely by STP tomography¹⁵. The main complementary strength of these efforts, however, comes from the broad range of tracers used. Given that each tracer has its own advantages and problems³³, the information derived from all three projects will ensure generalizable interpretation of the projection results throughout the brain. The CSHL group uses a combination of traditional anterograde and retrograde tracers, fluorophore-conjugated dextran amine (BDA)³⁴ and cholera toxin B (CTB) subunit³⁵, respectively, which are complemented by a combination of viral vector-based tracers, GFP-expressing adeno-associated virus (AAV)³⁶ for anterograde tracing (Figure 2a) and modified rabies virus²⁷ for retrograde tracing. While the virus-based methods are less tested, they offer advantages in terms of the brightness of labeling and the possibility of cell type-specific targeting using Cre-dependent viral vectors³⁷ and transgenic lines expressing the Cre recombinase enzyme under the control of cell type specific promoters^{38–40}. The AIBS team uses solely anterograde tracing by AAV-GFP viruses⁴¹ (Figure 2b), in many cases taking advantage of Cre driver mouse lines for cell type-specific labeling. Finally, the team at UCLA is using a strategy of two injections per brain, each with a mix of anterograde and retrograde tracers⁴², CTB together with Phaseolus vulgaris leucoagglutinin (PHA-L)⁴³ and FluoroGold (FG)⁴⁴ together with BDA^{42,45}. This approach has an added advantage since it allows direct visualization of the convergence of inputs and outputs from across different areas in one brain^{42,46,47}.

The unprecedented amounts of data being collected by these projects means that the significant person-hours historically spent performing microscopy have largely shifted toward data analysis. The first step of such data analysis comprises the compilation of the serial section images for viewing as whole-brain datasets at resolutions beyond the minimum geometric volume of the neuronal structures of interest—somata for retrograde and axons for anterograde tracing. All three projects offer a convenient way to browse the datasets online, including high-resolution zoom-in views that in most cases are sufficient for visual determination of labeled somata and axons. Importantly, all three projects use the Allen Mouse Brain Atlas for the registration of the coronal sections, which will provide

significant help in the cross-validation of results obtained from the different tracers. The Allen Mouse Brain Connectivity Atlas website also offers the option to view the data after projection segmentation, which selectively highlights labeled axons, as well as in 3D in the Brain Explorer registered to the Allen Mouse Brain Atlas⁴⁸ (Figure 2b).

The second step of data analysis requires the development of informatics methods for quantitation of the datasets, which will facilitate the interpretation of the online available data. The Allen Mouse Brain Connectivity Atlas online tools allow the user to search the projections between injected regions and display the labeled pathways as tracks in 3D in the Brain Explorer. The CSHL and UCLA connectomes can currently be viewed online as serial section datasets. The data from the Cre driver mouse lines in the AIBS project provide a unique feature of cell type specificity for the interpretation of the anterograde projections. The main strength of the CSHL and UCLA efforts lies in the multiplicity of the anatomical tracers utilized. The use of multiple retrograde tracers in particular will yield useful information, since retrogradely labeled somas ($> 10 \mu\text{m}$ in diameter) are easier to quantitate than thin ($< 1 \mu\text{m}$) axon fibers. These experiments will also provide an important comparison between the traditional CTB and FluoroGold tracers and the rabies virus-tracer that is also being used in transsynaptic labeling (see below), but is less studied and may show some variation in transport affinity at different types of synapses. In summary, the LM-based mesoscopic mapping projects are set to transform the study of the circuit wiring of the mouse brain by providing online access to whole-brain datasets from several thousand injections of anterograde and retrograde tracers. The informatics tools being developed to search the databases will greatly aid in parsing the large amounts of data and in accessing specific brain samples for detailed scholarly analyses by the neuroscience community.

Mapping connectivity using transsynaptic tracers

In contrast to EM methods, which provide a read-out of neuronal connectivity with synapse resolution over small volumes of tissue, the whole-brain LM methods permit the assessment of projection-based connectivity between brain regions and in some cases between specific cell types in those regions, but without the option to visualize the underlying synaptic contacts. Transsynaptic viruses that cross either multiple or single synapses can help to circumvent the requirement to confirm connectivity at the EM resolution, since such connectivity may be inferred from the known direction and mechanism of spread of the transsynaptic tracer. Transsynaptic tracers based on rabies (RV), pseudorabies (PRV), and herpes simplex (HSV) viruses, which repeatedly cross synaptic connections in a retrograde or anterograde direction, are powerful tools for elucidating multistep pathways up and downstream from the starter cell population^{49–51}. Furthermore, modified transsynaptic rabies viruses have been developed that are restricted in their spread to a single synaptic jump and thus can be used to identify monosynaptic connections onto and downstream of specific neuronal populations and even individual cells^{27,52–58}.

RV spreads from the initially infected cells in a transsynaptic retrograde manner^{49,59}. RV infection does not occur via spurious spread or uptake by fibers of passage and, since it cannot cross via electrical synapses, it is an effective tool for unidirectional anatomical tracing⁶⁰. In the modified RV system, the infection can also be cell type-targeted by encapsulating the glycoprotein-deficient rabies virus with an avian virus envelope protein (SAD-ΔG-EnvA). This restricts infection to only those cells that express an avian receptor gene (TVA), which is natively found in birds but not in mammals^{61,62}. Thus, the delivery of vectors driving the expression of both TVA and RV-G into a single cell^{28,56,54} (see below) or a specific population of cells^{55,63}, ensures that only the targeted cell/s will (i) be susceptible to initial infection and (ii) provide the replication-incompetent virus with RV-G required for trans-synaptic infection⁶⁴. In this system, the virus can spread from the

primarily infected cell/s to the presynaptic input cells, which become labeled by the fluorescent protein expression. However, since the presynaptic cells do not express RV-G²⁸, the virus cannot spread further. This approach thus allows the discovery of the identity and location of the upstream input network relative to a defined population of neurons^{57,58}.

Brain region- and cell type-specificity for mapping connectivity by the modified RV system can be achieved by using a Cre recombinase-dependent helper virus driving expression of TVA and RV-G and transgenic mouse lines that express Cre in specific cell types or cortical layers^{38,39,63}. This strategy is particularly useful for brain regions comprising many different cell types that could not be otherwise selectively targeted. Moreover, the engineering of other neurotropic transsynaptic viruses is adding new tools for anatomical tracing, including Cre-dependent anterograde tracers based on a modified H129 strain of HSV⁶⁵ and vesicular stomatitis virus⁶⁶, and retrograde tracers based on a modified pseudorabies virus (H. Oyibo and A. Zador, CSHL, personal communication). The use of retrograde and anterograde transsynaptic viruses, in combination with whole-brain LM methods, thus promises to afford unprecedented access to the upstream and downstream connectivity of specific cell types in the mouse brain.

Current challenges and opportunities for whole-brain LM methods

As highlighted above, LM instruments for whole-brain imaging are expected to make a significant contribution in large scale projects that focus on anatomical connectivity at the level of the whole mouse brain. It has also become clear that the use of these instruments will have an impact in many experimental applications in different neuroscience laboratories. It is therefore imperative that there exist broadly applicable image processing, warping and analytical tools that will facilitate data sharing and across-laboratory collaboration and validation in future neuroscience studies focusing on, for example, mapping whole-brain anatomical changes during development and in response to experience.

One practical problem arising from the choice to scan entire mouse brains at high resolution relates to the handling of large datasets (up to several TB per brain), which necessitates automated analytical pipelining. STP tomography is currently the most broadly used method among the whole-brain LM instruments and there are freely available informatics tools for compiling STP tomography image stacks and viewing them as three-dimensional data, including algorithms that automate seamless stitching¹⁵. Another key challenge for charting the distribution of the labeled elements in the whole mouse brain is the process of accurate registration of the individual brain datasets onto an anatomical reference atlas. To this end, scientists at AIBS have generated the open source segmented Allen Mouse Brain Atlas for the adult C57BL/6 mouse^{29,31,32,48}, which is also available for registration of datasets generated by STP tomography (Figure 2b and 4). In addition, the so-called Waxholm space (WHS) for standardized digital atlasing⁶⁷ allows comparisons of registered mouse brain data using multiple brain atlases, including the Allen Brain Atlas, the digital Paxinos and Franklin Mouse Brain Atlas⁶⁸, and several MRI reference mouse brains. The continuing development of the WHS and other online data analysis platforms^{30,69,70} will be essential for standardized comparisons of mouse brain data collected by different laboratories using different instruments.

The completion of the three mesoscopic connectome projects in the next several years will yield a comprehensive map of point-to-point connectivity between anatomical regions in the mouse brain⁷. Determining the cell-type identity of the neurons sending and receiving the connections in the brain regions will be essential for interpreting the function of the brainwide neural circuits. Immunohistochemical analyses of labeled circuits have proven

invaluable for ascertaining the identity of specific classes of neurons^{71–73} and synaptic connections^{52,74}. The combination of immunohistochemical analysis by array tomography^{75,76} and anatomical tracing by the whole-brain LM instruments promises to be particularly powerful, since it will bring together two largely automated methodologies with complementary focus on synaptic and mesoscopic connectivity, respectively. STP tomography outputs sectioned tissue (typically 50 μm thick sections¹⁵), which can be further resectioned, processed and re-imaged by array tomography for integrating cell type-specific information into the whole-brain datasets. Industrial-level automation of slice capture and immunostaining can be developed to minimize manual handling and enhance the integration of immunohistochemistry and STP tomography. In addition, sectioning and immunostaining can be also applied to LSMF imaged mouse brains²⁰.

A related, cell-type focused application of whole-brain LM imaging will be to quantitatively map the distribution (the cell counts) of different neuronal cell types in all anatomical regions in the mouse brain. Several such cell count-based anatomical studies have been done previously at smaller scales, revealing, for example, cell densities with respect to cortical vasculature⁷⁷ or the density of neuronal cell types per layers in a single cortical column^{78–80}. Using the whole brain LM methods, a comprehensive anatomical atlas of different GABAergic inhibitory interneurons⁸¹ can now be generated by imaging cell type-specific Cre knock-in mouse lines^{38,39} crossed with Cre-dependent reporter mice expressing nuclear GFP. These and similar datasets for other neuronal cell types will complement the mesoscopic brain region connectivity data and help the interpretation of the immunohistochemistry data by providing a reference for total numbers of specific cell types per anatomical brain regions.

Integrating brain anatomy and function

The anterograde, retrograde and transsynaptic tracing approaches described above will yield the structural scaffold of anatomical projections and connections throughout the mouse brain. However, such data will not be sufficient to identify how specific brain regions connect to form functional circuits driving different behaviors. Bridging whole-brain structure and function is the next frontier in systems neuroscience and the development of new technologies and methods will be crucial in achieving progress.

The structure-function relationship of single neurons can be examined by *in vivo* intracellular delivery of the DNA vectors required for targeting and driving transsynaptic virus expression via patch pipettes in loose cell-attached mode for electroporation⁵⁶ or via whole-cell recording⁵⁴ (Figure 3). Used in combination with two-photon microscopy, this single cell delivery technique may also be targeted at fluorescently labeled neurons of specific cell types^{56,82,83}. The whole-cell method is particularly informative, since its intracellular nature permits recording the intrinsic biophysical profile of the target cell, which, in turn, may reflect its functional connectivity status within the local network⁸⁴. In addition, by recording sensory-evoked inputs, it is possible to compare single cell synaptic receptive fields and anatomical local and long-range connectivity traced by LM methods⁵⁴. This combinatorial approach, involving single cell electrophysiology and genetic manipulation designed for connection mapping, makes it possible to test long-standing theories regarding the extent to which emergent features of sensory cortical function manifest via specific wiring motifs⁸⁵.

As has recently been achieved for serial EM-based reconstruction^{86,87}, it will also be valuable to functionally characterize larger local neuronal populations for registration against LM-based connectivity data. In this sense, genetically encoded calcium indicators, which permit physiological characterization of neuronal activity in specific cell types^{88–90},

alongside viral vectors for transsynaptic labeling and LM-based tracing will play critical complimentary roles. Large volume *in vivo* two-photon imaging of neuronal activity prior to *ex vivo* whole-brain imaging will establish the extent to which connectivity patterns relate to function⁹¹ at the level of single cells, local and long-range circuits. Interpolation of such experiments will be reliant on the ability to cross-register *in vivo* functional imaging with complete *ex vivo* LM connectivity data. Preliminary experiments, already hinting at the spatial spread of monosynaptic connectivity of individual principle cortical cells, suggest that combination of functional imaging and traditional anatomical circuit reconstruction may only be feasible at the local network level where connection probability is the highest^{92–94}. Given the broad, sparse expanse of connectivity in most brain regions and especially in cortical areas, high-throughput whole brain LM methods will be imperative for complete anatomical circuit reconstruction of the functionally characterized local networks.

The amalgamation of whole-brain LM and physiological methods for single neurons and small networks offers a powerful means to study the mouse brain. An exciting application of this approach will be to trace the synaptic circuits of neurons functionally characterized in head-fixed behaving animals engaged in tasks related to spatial navigation, sensorimotor integration and other complex brain functions^{95–97}. This research will lead to the generation of whole-brain structure-function hypotheses for specific behaviors, which can then be tested for causality by optogenetic methods targeted to the identified cell types and brain regions⁹⁸. Furthermore, the LM, physiological and optogenetic methods can be applied to interrogate entire brain systems in large scale projects, as is currently being done for the mouse visual cortex in an effort led by Christof Koch and R. Clay Reid at AIBS⁹⁹.

Finally, a discussion in the neuroscience community has been initiated regarding the feasibility of mapping activity at cellular resolution in whole brains and linking the identified activity patterns to brain anatomy¹⁰⁰. Today, such experiments are possible in small, transparent organisms, as was demonstrated by two-photon microscopy and LSM-based imaging of brain activity in larval zebrafish expressing the calcium indicator GCaMP^{89,101,102}. Understandably, LM-based approaches will not be useful for *in vivo* whole-brain imaging in larger, non-transparent animals and the invention of new disruptive technologies will likely be needed to achieve the goal of real-time brain activity mapping at cellular resolution in, for example, the mouse. On the other hand, LM methods can be used to map patterns of whole-brain activation indirectly, by post hoc visualization of activity-induced expression of immediate early genes (IEGs), such as *c-fos*, *Arc*, or *Homer 1a*¹⁰³. Transgenic fluorescent IEG-reporter mice, like *c-fos*-GFP or *Arc*-GFP mice^{104–106}, can be trained in a specific behavior, their brains subsequently imaged *ex-vivo*, and the exact distribution of GFP-positive neurons mapped and analyzed by computational methods (Figure 4). In this approach, a statistical analysis of the counts of GFP-labeled neurons can be used to identify brain regions and cell types activated during behaviors, but without providing an information on the temporal sequence of brain region activation or the firing patterns of the activated cells. However, the development of more sensitive, for instance, fluorescent RNA-based methods, may allow calibration of the cellular signal with respect to the temporal window and the pattern of activity related to the IEG induction. Such calibration would significantly enhance the power of LM-based whole-brain IEG mapping, which, in combination with the connectomic data, could then be used to begin to build cellular resolution models of function-based whole brain circuits.

Conclusions

The advances in automated LM methods, anatomical tracers, physiological methods and informatics tools have begun to transform our understanding of the circuit wiring in the mouse brain. The focus on the mouse as an animal model is, of course, not accidental. In

addition to the generation of cell type-specific knock-in mouse lines^{38–40} that allow the study of specific neuronal populations in the normal brain, mouse genetics are used in hundreds of laboratories to model gene mutations linked to heritable human disorders, including complex cognitive disorders such as autism and schizophrenia. Without doubt, understanding the relationships between brain structure and function in the genetic mouse models will be crucial to understanding the underlying brain circuit mechanisms of these disorders. The toolbox of LM methods described here, and the continuing development of new methods, promise to transform the study of brain circuits in animal models and to decipher the structure-function relationships essential to the understanding of complex brain functions and their deficits in human brain disorders.

Acknowledgments

We thank Partha Mitra, Hongkui Zeng and Christian Niedworok for comments on the manuscript and J. Kuhl for the graphics. PO is supported by the National Institute of Mental Health grant 1R01MH096946-01 and Simons Foundation for Autism Research grants 204719 and 253447. TWM is a Wellcome Trust Investigator and is supported by the Medical Research Council MC U1175975156.

References

1. Golgi C. Sulla struttura della sostanza grigia del cervello. *Gazz Med Ital (Lombardia)*. 1873; 33:244–246.
2. Ramón, Y.; Cajal, S. *Textura del sistema nervioso del hombre y de los vertebrados*. Vol. Vol. 2. Moya; 1904.
3. Felleman DJ, Van Essen DC. Distributed hierarchical processing in the primate cerebral cortex. *Cerebral cortex*. 1991; 1:1–47. [PubMed: 1822724]
4. Rockland KS, Pandya DN. Laminar origins and terminations of cortical connections of the occipital lobe in the rhesus monkey. *Brain research*. 1979; 179:3–20. [PubMed: 116716]
5. Milham M, et al. Human Connectome review. *Nature methods*. 2013; XX:X.
6. Helmstaedter M. Dense reconstruction by Moritz review. *Nature methods*. 2013; XX:X.
7. Bohland JW, et al. A proposal for a coordinated effort for the determination of brainwide neuroanatomical connectivity in model organisms at a mesoscopic scale. *PLoS computational biology*. 2009; 5:e1000334. [PubMed: 19325892] * This paper describes the rationale for mapping connectivity in the whole mouse brain at the mesoscale level by light microscopy.
8. Odgaard A, Andersen K, Melsen F, Gundersen HJ. A direct method for fast three-dimensional serial reconstruction. *Journal of microscopy*. 1990; 159:335–342. [PubMed: 2243366]
9. Ewald AJ, McBride H, Reddington M, Fraser SE, Kerschmann R. Surface imaging microscopy, an automated method for visualizing whole embryo samples in three dimensions at high resolution. *Dev Dyn*. 2002; 225:369–375. [PubMed: 12412023]
10. Tsai PS, et al. All-optical histology using ultrashort laser pulses. *Neuron*. 2003; 39:27–41. [PubMed: 12848930] * This study pioneered the approach of serial imaging by two-photon microscopy and tissue sectioning for *ex-vivo* collection of neuronanatomical data.
11. Sands GB, et al. Automated imaging of extended tissue volumes using confocal microscopy. *Microscopy research and technique*. 2005; 67:227–239. [PubMed: 16170824]
12. Ragan T, et al. High-resolution whole organ imaging using two-photon tissue cytometry. *Journal of biomedical optics*. 2007; 12:014015. [PubMed: 17343490]
13. Mayerich D, Abbott L, McCormick B. Knife-edge scanning microscopy for imaging and reconstruction of three-dimensional anatomical structures of the mouse brain. *Journal of microscopy*. 2008; 231:134–143. [PubMed: 18638197]
14. Li A, et al. Micro-optical sectioning tomography to obtain a high-resolution atlas of the mouse brain. *Science*. 2011; 330:1404–1408. [PubMed: 21051596]
15. Ragan T, et al. Serial two-photon tomography for automated ex vivo mouse brain imaging. *Nature methods*. 2012; 9:255–258. [PubMed: 22245809] * This study introduces the method of STP tomography and demonstrates its use for anterograde and retrograde tracing in the mouse brain.

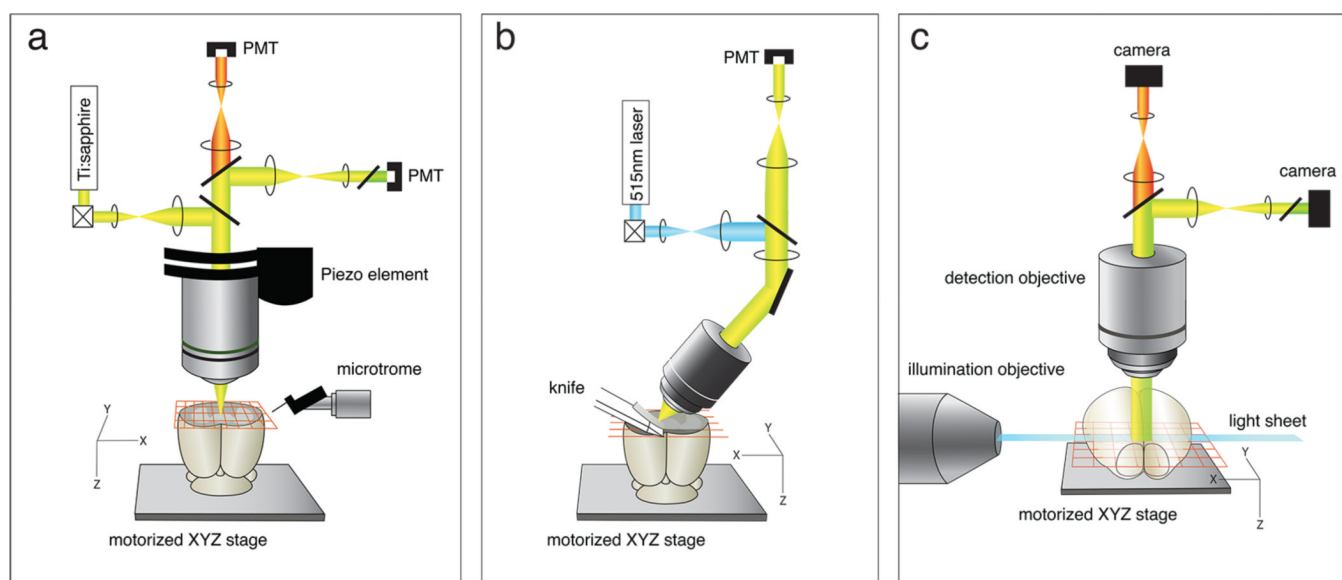
16. Gong H, et al. Continuously Tracing Brain-wide Long-distance Axonal Projections in Mice at a One-micron Voxel Resolution. *NeuroImage*. 2013 * This study demonstrates the first long-range tracing of individual axons in the mouse brain by the fMOST method.
17. Denk W, Strickler JH, Webb WW. Two-photon laser scanning fluorescence microscopy. *Science*. 1990; 248:73–76. [PubMed: 2321027]
18. Huisken J, Swoger J, Del Bene F, Wittbrodt J, Stelzer EH. Optical sectioning deep inside live embryos by selective plane illumination microscopy. *Science*. 2004; 305:1007–1009. [PubMed: 15310904]
19. Dödt HU, et al. Ultramicroscopy: three-dimensional visualization of neuronal networks in the whole mouse brain. *Nature methods*. 2007; 4:331–336. [PubMed: 17384643] * This study is the first to demonstrate the use of LSFM for imaging the entire mouse brain.
20. Niedworok CJ, et al. Charting monosynaptic connectivity maps by two-color light-sheet fluorescence microscopy. *Cell Rep*. 2012; 2:1375–1386. [PubMed: 23142666]
21. Chung K, et al. Structural and molecular interrogation of intact biological systems. *Nature*. 2013
22. Deisseroth K. Perspective on CLARITY. *Nat Meth*. 2013; XX:XX.
23. Leischner U, Zieglansberger W, Dödt HU. Resolution of ultramicroscopy and field of view analysis. *PLoS ONE*. 2009; 4:e5785. [PubMed: 19492052]
24. Mertz J, Kim J. Scanning light-sheet microscopy in the whole mouse brain with HiLo background rejection. *Journal of biomedical optics*. 2010; 15:016027. [PubMed: 20210471]
25. Kalchmair S, Jahrling N, Becker K, Dödt HU. Image contrast enhancement in confocal ultramicroscopy. *Optics letters*. 2010; 35:79–81. [PubMed: 20664679]
26. Keller PJ, et al. Fast, high-contrast imaging of animal development with scanned light sheet-based structured-illumination microscopy. *Nature methods*. 2010; 7:637–642. [PubMed: 20601950]
27. Wickersham IR, Finke S, Conzelmann KK, Callaway EM. Retrograde neuronal tracing with a deletion-mutant rabies virus. *Nature methods*. 2007; 4:47–49. [PubMed: 17179932]
28. Wickersham IR, et al. Monosynaptic restriction of transsynaptic tracing from single, genetically targeted neurons. *Neuron*. 2007; 53:639–647. [PubMed: 17329205] * This study describes a genetically modified rabies virus designed to specifically label direct presynaptic input onto a given cell population.
29. Ng L, et al. An anatomic gene expression atlas of the adult mouse brain. *Nature neuroscience*. 2009; 12:356–362.
30. Jones EG, Stone JM, Karten HJ. High-resolution digital brain atlases: a Hubble telescope for the brain. *Annals of the New York Academy of Sciences*. 2011; 1225(Suppl 1):E147–E159. [PubMed: 21599693]
31. Lein ES, et al. Genome-wide atlas of gene expression in the adult mouse brain. *Nature*. 2007; 445:168–176. [PubMed: 17151600] * This study pioneered large scale LM-based whole-brain anatomy and introduced the Allen Mouse Brain Atlas and online data portal.
32. Dong, HW. The Allen reference atlas: A digital color brain atlas of the C57Bl/6J male mouse. John Wiley & Sons Inc; 2008.
33. Lanciego JL, Wouterlood FG. A half century of experimental neuroanatomical tracing. *J Chem Neuroanat*. 2011; 42:157–183. [PubMed: 21782932]
34. Glover JC, Petursdottir G, Jansen JK. Fluorescent dextran-amines used as axonal tracers in the nervous system of the chicken embryo. *Journal of neuroscience methods*. 1986; 18:243–254. [PubMed: 2432362]
35. Llewellyn-Smith IJ, Martin CL, Arnold LF, Minson JB. Tracer-toxins: cholera toxin B-saporin as a model. *Journal of neuroscience methods*. 2000; 103:83–90. [PubMed: 11074098]
36. Grinevich V, Brecht M, Osten P. Monosynaptic pathway from rat vibrissa motor cortex to facial motor neurons revealed by lentivirus-based axonal tracing. *J Neurosci*. 2005; 25:8250–8258. [PubMed: 16148232]
37. Atasoy D, Aponte Y, Su HH, Sternson SM. A FLEX switch targets Channelrhodopsin-2 to multiple cell types for imaging and long-range circuit mapping. *The Journal of neuroscience : the official journal of the Society for Neuroscience*. 2008; 28:7025–7030. [PubMed: 18614669]

38. Taniguchi H, et al. A Resource of Cre Driver Lines for Genetic Targeting of GABAergic Neurons in Cerebral Cortex. *Neuron*. 2011; 71:995–1013. [PubMed: 21943598]
39. Madisen L, et al. A robust and high-throughput Cre reporting and characterization system for the whole mouse brain. *Nature neuroscience*. 2010; 13:133–140.
40. Madisen L, et al. A toolbox of Cre-dependent optogenetic transgenic mice for light-induced activation and silencing. *Nature neuroscience*. 2012; 15:793–802.
41. Harris JA, Wook Oh S, Zeng H. Adeno-associated viral vectors for anterograde axonal tracing with fluorescent proteins in nontransgenic and cre driver mice. *Current protocols in neuroscience / editorial board, Jacqueline N Crawley ... [et al]*. 2012; Chapter 1(Unit 1 20):21–18.
42. Thompson RH, Swanson LW. Hypothesis-driven structural connectivity analysis supports network over hierarchical model of brain architecture. *Proceedings of the National Academy of Sciences of the United States of America*. 2010; 107:15235–15239. [PubMed: 20696892]
43. Gerfen CR, Sawchenko PE. An anterograde neuroanatomical tracing method that shows the detailed morphology of neurons, their axons and terminals: immunohistochemical localization of an axonally transported plant lectin, Phaseolus vulgaris leucoagglutinin (PHA-L). *Brain research*. 1984; 290:219–238. [PubMed: 6198041]
44. Naumann T, Hartig W, Frotscher M. Retrograde tracing with Fluoro-Gold: different methods of tracer detection at the ultrastructural level and neurodegenerative changes of back-filled neurons in long-term studies. *Journal of neuroscience methods*. 2000; 103:11–21. [PubMed: 11074092]
45. Reiner A, et al. Pathway tracing using biotinylated dextran amines. *Journal of neuroscience methods*. 2000; 103:23–37. [PubMed: 11074093]
46. Hintiryan H, et al. Comprehensive connectivity of the mouse main olfactory bulb: analysis and online digital atlas. *Front Neuroanat*. 2012; 6:30. [PubMed: 22891053]
47. Conte WL, Kamishina H, Reep RL. Multiple neuroanatomical tract-tracing using fluorescent Alexa Fluor conjugates of cholera toxin subunit B in rats. *Nat Protoc*. 2009; 4:1157–1166. [PubMed: 19617887]
48. Sunkin SM, et al. Allen Brain Atlas: an integrated spatio-temporal portal for exploring the central nervous system. *Nucleic acids research*. 2013; 41:D996–D1008. [PubMed: 23193282]
49. Ugolini G. Advances in viral transneuronal tracing. *Journal of neuroscience methods*. 2010; 194:2–20. [PubMed: 20004688]
50. Ekstrand MI, Enquist LW, Pomeranz LE. The alpha-herpesviruses: molecular pathfinders in nervous system circuits. *Trends Mol Med*. 2008; 14:134–140. [PubMed: 18280208]
51. Song CK, Enquist LW, Bartness TJ. New developments in tracing neural circuits with herpesviruses. *Virus Res*. 2005; 111:235–249. [PubMed: 15893400]
52. Callaway EM. Transneuronal circuit tracing with neurotropic viruses. *Current opinion in neurobiology*. 2008; 18:617–623. [PubMed: 19349161]
53. Wickersham IR, Feinberg EH. New technologies for imaging synaptic partners. *Current opinion in neurobiology*. 2012; 22:121–127. [PubMed: 22221865]
54. Rancz EA, et al. Transfection via whole-cell recording in vivo: bridging single-cell physiology, genetics and connectomics. *Nature neuroscience*. 2011; 14:527–532. * This study is the first to combine intracellular neuronal recording with DNA delivery. The authors use this method to map the synaptic function of a single cell *in vivo* then target rabies-based retrograde labelling of the cells synaptic input.
55. Miyamichi K, et al. Cortical representations of olfactory input by trans-synaptic tracing. *Nature*. 2011; 472:191–196. [PubMed: 21179085]
56. Marshel JH, Mori T, Nielsen KJ, Callaway EM. Targeting single neuronal networks for gene expression and cell labeling in vivo. *Neuron*. 2010; 67:562–574. [PubMed: 20797534] * This paper describes an electroporation method for single cell delivery of DNA for targeted infection of modified rabies virus.
57. Takatoh J, et al. New modules are added to vibrissal premotor circuitry with the emergence of exploratory whisking. *Neuron*. 2013; 77:346–360. [PubMed: 23352170]
58. Arenkiel BR, et al. Activity-induced remodeling of olfactory bulb microcircuits revealed by monosynaptic tracing. *PLoS ONE*. 2011; 6:e29423. [PubMed: 22216277]

59. Finke S, Conzelmann KK. Replication strategies of rabies virus. *Virus Res.* 2005; 111:120–131. [PubMed: 15885837]
60. Ugolini G. Specificity of rabies virus as a transneuronal tracer of motor networks: transfer from hypoglossal motoneurons to connected second-order and higher order central nervous system cell groups. *The Journal of comparative neurology.* 1995; 356:457–480. [PubMed: 7642806]
61. Federspiel MJ, Bates P, Young JA, Varmus HE, Hughes SH. A system for tissue-specific gene targeting: transgenic mice susceptible to subgroup A avian leukosis virus-based retroviral vectors. *Proceedings of the National Academy of Sciences of the United States of America.* 1994; 91:11241–11245. [PubMed: 7972042]
62. Young JA, Bates P, Varmus HE. Isolation of a chicken gene that confers susceptibility to infection by subgroup A avian leukosis and sarcoma viruses. *Journal of virology.* 1993; 67:1811–1816. [PubMed: 8383211]
63. Wall NR, Wickersham IR, Cetin A, De La Parra M, Callaway EM. Monosynaptic circuit tracing in vivo through Cre-dependent targeting and complementation of modified rabies virus. *Proceedings of the National Academy of Sciences of the United States of America.* 2010; 107:21848–21853. [PubMed: 21115815]
64. Etessami R, et al. Spread and pathogenic characteristics of a G-deficient rabies virus recombinant: an in vitro and in vivo study. *J Gen Virol.* 2000; 81:2147–2153. [PubMed: 10950970]
65. Lo L, Anderson DJ. A Cre-dependent, anterograde transsynaptic viral tracer for mapping output pathways of genetically marked neurons. *Neuron.* 2011; 72:938–950. [PubMed: 22196330]
66. Beier KT, et al. Anterograde or retrograde transsynaptic labeling of CNS neurons with vesicular stomatitis virus vectors. *Proceedings of the National Academy of Sciences of the United States of America.* 2011; 108:15414–15419. [PubMed: 21825165]
67. Hawrylycz M, et al. Digital atlasing and standardization in the mouse brain. *PLoS computational biology.* 2011; 7:e1001065. [PubMed: 21304938]
68. Paxinos, G.; Franklin, KB. *The mouse brain in stereotaxic coordinates.* Gulf Professional Publishing; 2004.
69. Swanson LW, Bota M. Foundational model of structural connectivity in the nervous system with a schema for wiring diagrams, connectome, and basic plan architecture. *Proceedings of the National Academy of Sciences of the United States of America.* 2010; 107:20610–20617. [PubMed: 21078980]
70. Moene IA, Subramaniam S, Darin D, Leergaard TB, Bjaalie JG. Toward a workbench for rodent brain image data: systems architecture and design. *Neuroinformatics.* 2007; 5:35–58. [PubMed: 17426352]
71. Klausberger T, Somogyi P. Neuronal diversity and temporal dynamics: the unity of hippocampal circuit operations. *Science.* 2008; 321:53–57. [PubMed: 18599766]
72. O'Rourke NA, Weiler NC, Micheva KD, Smith SJ. Deep molecular diversity of mammalian synapses: why it matters and how to measure it. *Nature reviews. Neuroscience.* 2012; 13:365–379.
73. Defelipe J, et al. New insights into the classification and nomenclature of cortical GABAergic interneurons. *Nature reviews. Neuroscience.* 2013; 14:202–216.
74. Emes RD, Grant SG. Evolution of synapse complexity and diversity. *Annual review of neuroscience.* 2012; 35:111–131.
75. Micheva KD, Busse B, Weiler NC, O'Rourke N, Smith SJ. Single-synapse analysis of a diverse synapse population: proteomic imaging methods and markers. *Neuron.* 2010; 68:639–653. [PubMed: 21092855]
76. Micheva KD, Smith SJ. Array tomography: a new tool for imaging the molecular architecture and ultrastructure of neural circuits. *Neuron.* 2007; 55:25–36. [PubMed: 17610815]
77. Tsai PS, et al. Correlations of neuronal and microvascular densities in murine cortex revealed by direct counting and colocalization of nuclei and vessels. *The Journal of neuroscience : the official journal of the Society for Neuroscience.* 2009; 29:14553–14570. [PubMed: 19923289]
78. Oberlaender M, et al. Cell type-specific three-dimensional structure of thalamocortical circuits in a column of rat vibrissa cortex. *Cerebral cortex.* 2012; 22:2375–2391. [PubMed: 22089425]

79. Meyer HS, et al. Inhibitory interneurons in a cortical column form hot zones of inhibition in layers 2 and 5A. *Proceedings of the National Academy of Sciences of the United States of America*. 2011; 108:16807–16812. [PubMed: 21949377]
80. Meyer HS, et al. Number and laminar distribution of neurons in a thalamocortical projection column of rat vibrissa cortex. *Cerebral cortex*. 2010; 20:2277–2286. [PubMed: 20534784]
81. Ascoli GA, et al. Petilla terminology: nomenclature of features of GABAergic interneurons of the cerebral cortex. *Nature reviews. Neuroscience*. 2008; 9:557–568.
82. Margrie TW, et al. Targeted whole-cell recordings in the mammalian brain in vivo. *Neuron*. 2003; 39:911–918. [PubMed: 12971892]
83. Kitamura K, Judkewitz B, Kano M, Denk W, Hausser M. Targeted patch-clamp recordings and single-cell electroporation of unlabeled neurons in vivo. *Nature methods*. 2008; 5:61–67. [PubMed: 18157136]
84. Angelo K, et al. A biophysical signature of network affiliation and sensory processing in mitral cells. *Nature*. 2012; 488:375–378. [PubMed: 22820253]
85. Reid RC. From functional architecture to functional connectomics. *Neuron*. 2012; 75:209–217. [PubMed: 22841307]
86. Briggman KL, Helmstaedter M, Denk W. Wiring specificity in the direction-selectivity circuit of the retina. *Nature*. 2011; 471:183–188. [PubMed: 21390125]
87. Bock DD, et al. Network anatomy and in vivo physiology of visual cortical neurons. *Nature*. 2011; 471:177–182. [PubMed: 21390124]
88. Wallace DJ, et al. Single-spike detection in vitro and in vivo with a genetic Ca²⁺ sensor. *Nature methods*. 2008; 5:797–804. [PubMed: 19160514]
89. Akerboom J, et al. Optimization of a GCaMP calcium indicator for neural activity imaging. *The Journal of neuroscience : the official journal of the Society for Neuroscience*. 2012; 32:13819–13840. [PubMed: 23035093]
90. Mank M, et al. A genetically encoded calcium indicator for chronic in vivo two-photon imaging. *Nature methods*. 2008; 5:805–811. [PubMed: 19160515]
91. Ko H, et al. Functional specificity of local synaptic connections in neocortical networks. *Nature*. 2011; 473:87–91. [PubMed: 21478872]
92. Holmgren C, Harkany T, Svennenfors B, Zilberter Y. Pyramidal cell communication within local networks in layer 2/3 of rat neocortex. *The Journal of physiology*. 2003; 551:139–153. [PubMed: 12813147]
93. Thomson AM, West DC, Wang Y, Bannister AP. Synaptic connections and small circuits involving excitatory and inhibitory neurons in layers 2–5 of adult rat and cat neocortex: triple intracellular recordings and biocytin labelling in vitro. *Cerebral cortex*. 2002; 12:936–953. [PubMed: 12183393]
94. Song S, Sjöström PJ, Reigl M, Nelson S, Chklovskii DB. Highly nonrandom features of synaptic connectivity in local cortical circuits. *PLoS biology*. 2005; 3:e68. [PubMed: 15737062]
95. Harvey CD, Collman F, Dombeck DA, Tank DW. Intracellular dynamics of hippocampal place cells during virtual navigation. *Nature*. 2009; 461:941–946. [PubMed: 19829374] * This study introduced the method of physiological recording in head-restrained mice on a spherical treadmill performing spatial tasks in virtual environment.
96. Harvey CD, Coen P, Tank DW. Choice-specific sequences in parietal cortex during a virtual-navigation decision task. *Nature*. 2012; 484:62–68. [PubMed: 22419153]
97. Huber D, et al. Multiple dynamic representations in the motor cortex during sensorimotor learning. *Nature*. 2012; 484:473–478. [PubMed: 22538608]
98. Fenno L, Yizhar O, Deisseroth K. The development and application of optogenetics. *Annual review of neuroscience*. 2011; 34:389–412.
99. Koch C, Reid RC. Neuroscience: Observatories of the mind. *Nature*. 2012; 483:397–398. [PubMed: 22437592]
100. Alivisatos AP, et al. Neuroscience. The brain activity map. *Science*. 2013; 339:1284–1285. [PubMed: 23470729]

101. Ahrens MB, Keller PJ. Whole-brain functional imaging at cellular resolution using light-sheet microscopy. *Nature methods*. 2013
102. Ahrens MB, et al. Brain-wide neuronal dynamics during motor adaptation in zebrafish. *Nature*. 2012; 485:471–477. [PubMed: 22622571]
103. Herrera DG, Robertson HA. Activation of c-fos in the brain. *Progress in neurobiology*. 1996; 50:83–107. [PubMed: 8971979]
104. Barth AL, Gerkin RC, Dean KL. Alteration of neuronal firing properties after in vivo experience in a FosGFP transgenic mouse. *J Neurosci*. 2004; 24:6466–6475. [PubMed: 15269256]
105. Grinevich V, et al. Fluorescent Arc/Arg3.1 indicator mice: a versatile tool to study brain activity changes in vitro and in vivo. *Journal of neuroscience methods*. 2009; 184:25–36. [PubMed: 19628007]
106. Reijmers LG, Perkins BL, Matsuo N, Mayford M. Localization of a stable neural correlate of associative memory. *Science*. 2007; 317:1230–1233. [PubMed: 17761885]

**Figure 1.**

Whole-brain LM methods. (a) STP tomography. Two-photon microscope is used to image the mouse brain in a coronal plane in a mosaic grid pattern and microtome sections off the imaged tissue. Piezo objective scanner can be used for z-stack imaging (image adapted from Ragan et al.¹⁵). (b) fMOST. Confocal line-scan is used to image the brain as 1 μm thin section cut by diamond knife (image adapted from Gong et al.¹⁶). (c) LSFM. The cleared brain is illuminated from the side with the light sheet (blue) through an illumination objective (or cylinder lens¹⁹) and imaged in a mosaic grid pattern from top (image adapted from Niedworok et al.²⁰). In all instruments, the brain is moved under the objective on motorized XYZ stage; PMT, photomultiplier tube.

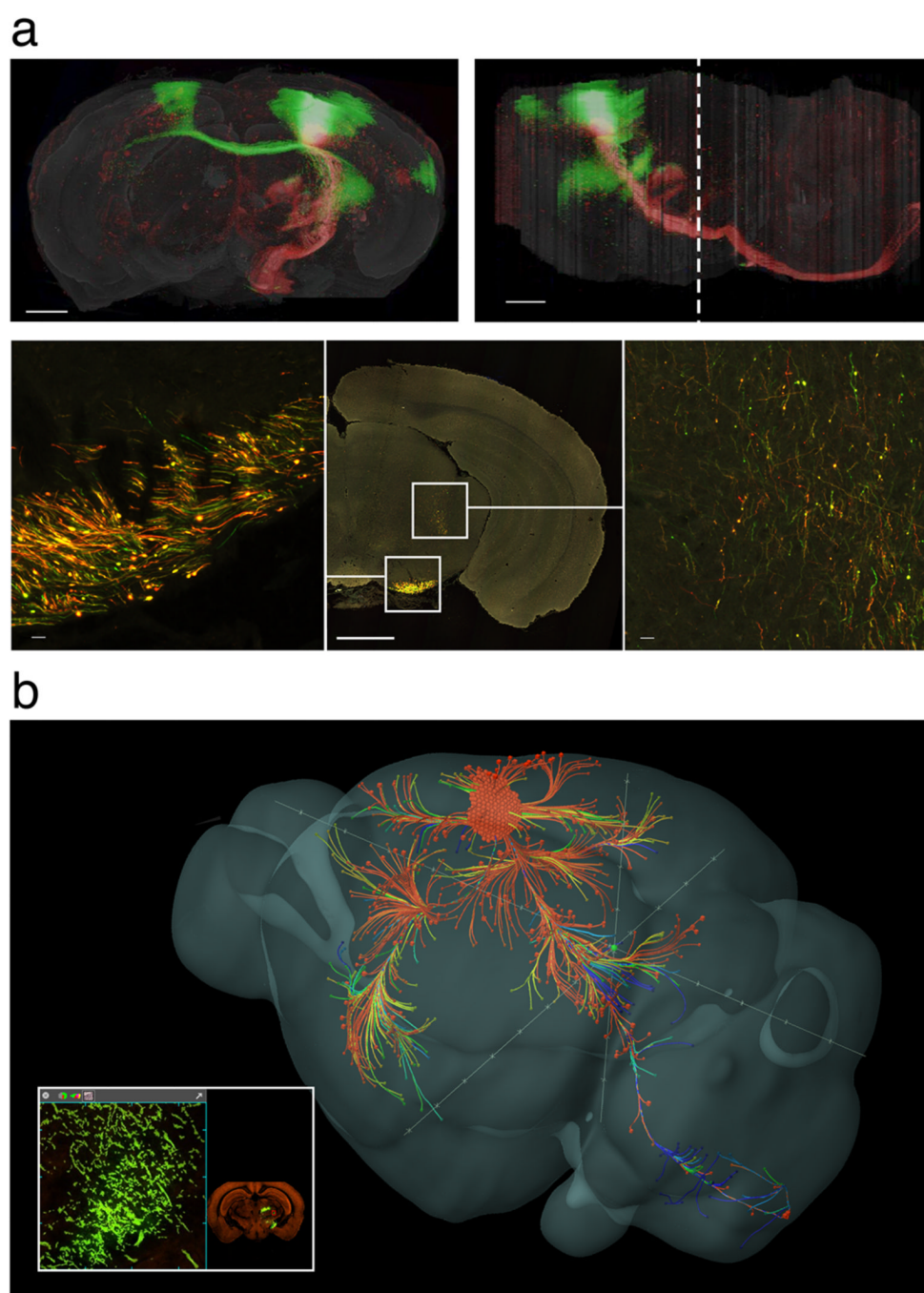
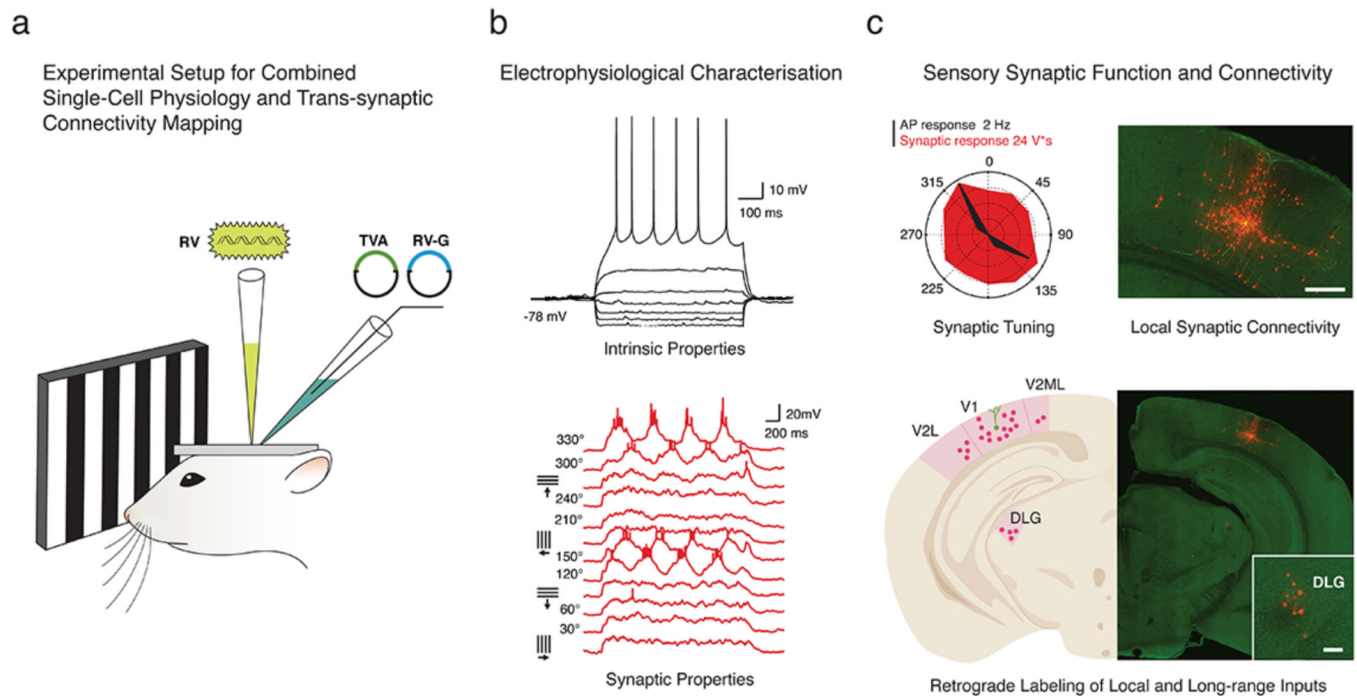


Figure 2.

Primary motor cortex (MOp) projection maps. (a) Mouse Brain Architecture (<http://brainarchitecture.org>) data of AAV-GFP injected into the supragranular layers and AAV-RFP injected in the infragranular layers (F. Mechler and P. Mitra, CSHL, unpublished data). Top panels show frontal (left) and lateral (right) views of the volume-rendered brain (scale bars = 1000 μ m); bottom panels show high-zoom views of the regions highlighted in the central image: axonal fibers in the cerebral peduncle (left) and projections to the midbrain reticular nucleus (right) (scale bar = 20 μ m). (b) Mouse Connectivity (<http://connectivity.brain-map.org>) data of a similar AAV-GFP injection show the MOp projectome reconstructed in the Allen Brain Explorer⁴⁸ (H. Zeng, AIBS, unpublished data).

The lower left inset shows high-zoom view and coronal section overview of projections in the ventral posteromedial nucleus of the thalamus (VPM)..

**Figure 3.**

Mapping the function and connectivity of single cells in the mouse brain *in vivo*. a) Patch pipettes—with internal solutions containing DNA vectors used to drive the expression of the TVA and RV-G proteins—are used to perform a whole-cell recording of the intrinsic and sensory-evoked synaptic properties of a single Layer 5 neuron in primary visual cortex (b). Following the recording, the encapsulated modified rabies virus is injected into the brain in close proximity to the recorded neuron. c) After a period of up to 12 days that ensures retrograde spread of the modified rabies from the recorded neuron, the brain is removed and imaged for identification of the local and long-range presynaptic inputs underlying the tuning of the recorded neuron to the direction of visual motion (polar plot). (top and bottom scale bar = 300 and 50 μm , respectively) Images modified from Rancz et al., 2011⁵⁴.

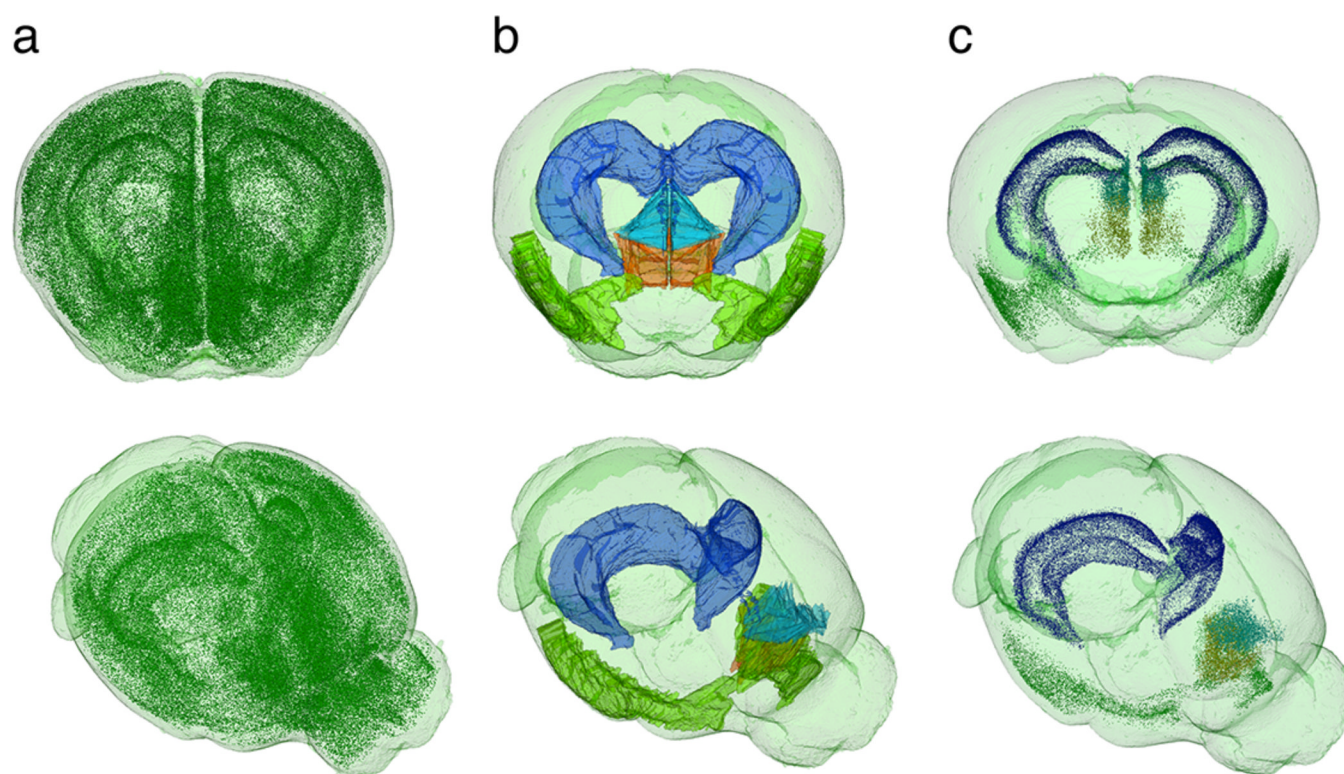


Figure 4.

Imaging c-fos induction as a means to map whole-brain activation. (a) 3D visualization of 367,378 c-fos-GFP cells detected in 280 coronal sections of an STP tomography dataset of a mouse brain after novelty exploration. (b) Examples of anatomical segmentation of the brain volume with the Allen Mouse Brain Reference Atlas labels⁴⁸ modified for the 280-section STP tomography datasets: hippocampus (blue), prelimbic (aqua blue), infralimbic (orange) and piriform (green) cortex. (c) Visualization of c-fos-GFP cells in the hippocampus (38,170 cells), prelimbic (3,305 cells), infralimbic (3,827 cells) and piriform (10,910 cells) cortex (P. Osten, Y. Kim, K. Umadevi Venkataraju, CSHL, unpublished data).